Resource-Efficient Technologies 3 (2017) 329–336

Contents lists available at ScienceDirect

Resource-Efficient Technologies

journal homepage: www.elsevier.com/locate/reffit

Optimization of adsorptive removal of α-toluic acid by CaO_2 nanoparticles using response surface methodology ☆

Sapana S. Madan, Kailas L. Wasewar*, C. Ravi Kumar

Advance Separation and Analytical Laboratory (ASAL), Department of Chemical Engineering, Visvesvaraya National Institute of Technology (VNIT), Nagpur, Maharashtra 440010, India

ARTICLE INFO

Article history:
Received 10 November 2016
Revised 16 February 2017
Accepted 7 March 2017
Available online 18 April 2017

Keywords:
Central composite design (CCD)
Analysis of variance (ANOVA)
Response surface methodology (RSM)
Calcium peroxide
Nanoparticles
Adsorption
α-Toluic acid

ABSTRACT

The present work addresses the optimization of process parameters for adsorptive removal of α-toluic acid by calcium peroxide (CaO_2) nanoparticles using response surface methodology (RSM). CaO_2 nanoparticles were synthesized by chemical precipitation method and confirmed by Transmission electron microscopy (TEM) and high-resolution TEM (HRTEM) analysis which shows the CaO_2 nanoparticles size range of 5–15 nm. A series of batch adsorption experiments were performed using CaO_2 nanoparticles to remove α-toluic acid from the aqueous solution. Further, an experimental based central composite design (CCD) was developed to study the interactive effect of CaO_2 adsorbent dosage, initial concentration of α-toluic acid, and contact time on α-toluic acid removal efficiency (response) and optimization of the process. Analysis of variance (ANOVA) was performed to determine the significance of the individual and the interactive effects of variables on the response. The model predicted response showed a good agreement with the experimental response, and the coefficient of determination, (R^2) was 0.92. Among the variables, the interactive effect of adsorbent dosage and the initial α-toluic acid concentration was found to have more influence on the response than the contact time. Numerical optimization of process by RSM showed the optimal adsorbent dosage, initial concentration of α-toluic acid, and contact time as 0.03 g, 7.06 g/L, and 34 min respectively. The predicted removal efficiency was 99.50%. The experiments performed under these conditions showed α-toluic acid removal efficiency up to 98.05%, which confirmed the adequacy of the model prediction.

1. Introduction

In recent years, the removal of organic pollutants and valuable chemicals from the aquatic environment and waste solutions has received a great interest. α-Toluic acid (phenylacetic acid) is an organic compound with a phenyl functional group and a carboxylic acid functional group. It is being produced by the hydrolysis of benzyl cyanide [1,2] and catabolic activities of the microorganism from various synthetic and natural aromatic compounds, such as aromatic amino acids, lignin, styrene, etc. [3]. α-Toluic acid is extensively used in the biotechnology and pharmaceutical industries for the production of β-lactam, antibiotics, penicillin G, etc. [4]. It has a wide range of biological activity, antibacterial, analgesic, and virucidal properties [5]. It can be produced by the fermentation of soya beans using *Bacillus licheniformis* [6,7]. The chemical structure of α-toluic acid is shown in Fig. 1. Its presence in water causes objectionable odor and harmful effects to the aquatic lives. Therefore, α-toluic acid has to be removed from water through a suitable technique. It is commonly removed from the waste streams by various methods such as precipitation, distillation, membrane separation, adsorption, reactive extraction, reverse osmosis, etc. [8]. Among these, adsorption is considered as a more feasible and reliable technique due to its high recovery, ease of operation, cost-effectiveness and less processing time [9].

Nanoadsorbents, nanocatalysts, nanopowders, nanotubes, nanostructured catalytic membranes, etc. have been widely used to resolve a lot of problems related to water treatments [10]. In particular, nanoparticles have been widely used as adsorbents

---

☆ Peer review under responsibility of Tomsk Polytechnic University.

* Corresponding author. Advance Separation and Analytical Laboratory (ASAL), Department of Chemical Engineering, Visvesvaraya National Institute of Technology (VNIT), Nagpur, Maharashtra 440010, India. Tel.: +91 712 2801561; fax: +91 712 2801565.

E-mail addresses: k_wasewar@rediffmail.com, klwasewar@che.vnit.ac.in (K.L. Wasewar).

https://doi.org/10.1016/j.reffit.2017.03.004

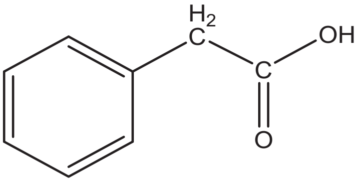

Fig. 1. Chemical structure of α-toluic acid.

due to their higher surface to the volume ratio [11], which can improve the adsorption capacity [12]. Calcium peroxide is white or yellowish solid peroxide, considered as temperature stable inorganic peroxide. It has been used as adsorbents for the removal of arsenic from wastewater, removal of toluene from petroleum products, and cleanup of oil spills, etc. [13–15].

The conventional method of optimization of the adsorption process involves multiple experiments to determine the optimal conditions showing maximum adsorption or removal efficiency [16]. Process optimization using the conventional approach of one factor at a time (OFAT) involves variation of one parameter at a time while other parameters are involved at an unspecified constant level [17]. It does not represent the combined effect of all the factors involved. The limitation of OFAT method can be eliminated by optimizing all the affecting parameters collectively by using the statistical experimental design. Response surface methodology (RSM) is one of the statistical techniques widely used to (i) design experiments, (ii) study the interactive effect of various parameters on the response, and (iii) predict the optimum conditions to showing a maximum response [18]. It is very useful for the enlargement of a process by improving the yield, reducing time, and lowering the operational cost [19]. The multiple regression analysis in the RSM helps to build a model that represents the actual experimental response. The analysis of variance (ANOVA) is incorporated in the RSM to evaluate the adequacy of the model and to test the significance of the model terms [18,20]. This method is appropriate for fitting a non-linear quadratic correlation, and for calculating the response surface correlation between the input and obtained parameters [20].

To the best of our knowledge, the literature on optimization of α-toluic acid adsorption process by RSM is not available. This is a first of its kind experimental study that deals with optimization of the adsorption of α-toluic acid using CaO_2 nanoparticles as adsorbent using RSM. In the present work, optimization of the process was carried using RSM to study the interactive effects of independent variables on α-toluic acid removal efficiency (response). The RSM predicted response was compared with our experimental data to understand the predictive capacity of the model. Fig. 2 shows the detailed structure of the overall present work.

2. Experimental

2.1. Materials

α-Toluic acid (98.5%) was received from Acros organics, New Jersey, USA. Calcium chloride ($CaCl_2$, 99.5%), hydrogen peroxide (H_2O_2, 35%), polyethylene glycol (PEG 200) solution, ammonia ($NH_3.H_2O$, 25%) solution, and sodium hydroxide (NaOH) were received from Merck, India. All the chemicals were used as received without purification. Double Distilled water obtained from Double Distillation unit (Remi India Ltd.) was used to prepare the aqueous solutions. 0.1 M NaOH was used to adjust the pH of the aqueous solutions.

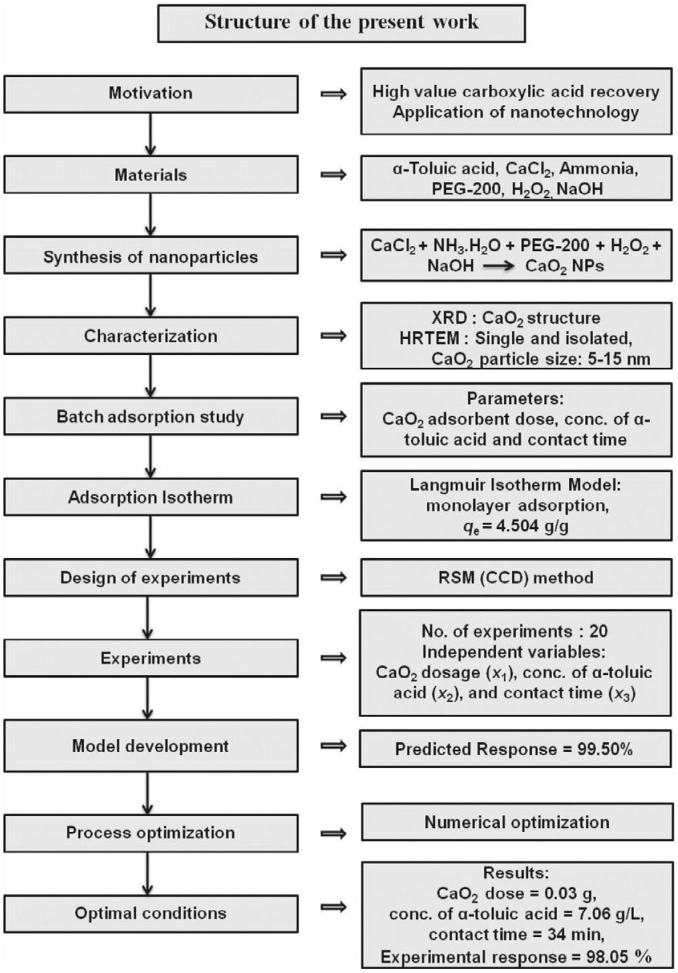

Fig. 2. Structure of the present work.

2.2. Equipment

X-Ray Diffractometer (XRD) [PANalytical X'pert Pro] analysis of the particles was performed in the range 20° to 70° (2θ range) with a step size of 0.01° using Cu target ($\lambda = 1.5406$ Å). Transmission Electron Microscopy (TEM) analysis of particles was performed in PHILIPS-CM 200, operated at 20–200 kV. High Resolution transmission electron microscopy (HRTEM) of particles was performed using JEOL JEM-2100. A digital pH meter (Spectral Lab Instrumental Pvt. Ltd., India) was used to measure the pH.

2.3. Synthesis of CaO_2 nanoparticles

The detailed CaO_2 nanoparticle synthesis procedure is given in our earlier article [21] and elsewhere [13,22]. Briefly, 3 g $CaCl_2$ was first dissolved in 30 mL water, followed by addition of 15 mL $NH_3.H_2O$ (1 M) and 120 mL PEG-200 solution. The mixture was allowed to stir at 250 rpm, and 15 mL H_2O_2 was immediately added to it at the rate of three drops per minute for about 1 h. The stirring was continued, and the pH of the mixture was adjusted to 11.5. The formation of CaO_2 nanoparticles was indicated by the change in color of the suspension from yellow to white. The suspension was centrifuged at 10,000 rpm for 5 min, and the CaO_2 nanoparticles were collected. Finally, the particles were washed thrice using 0.1 M NaOH solution, and then twice with distilled water, and dried at 80 °C for 120 min in a vacuum oven. The dried CaO_2 nanoparticles were later used for the adsorption experiments.

Few milligrams of the dried particles were used for characterization by XRD, TEM, and HRTEM.

2.4. Adsorption study

Batch adsorption experiments for the removal of α-toluic acid from aqueous solutions using CaO_2 nanoadsorbent were designed using response surface methodology using Design Expert (7.0.0) software (trial version). The interactive effects of CaO_2 adsorbent dosage, initial α-toluic acid concentration, and contact time on the α-toluic acid removal efficiency were studied in the range of 0.008–0.03 g, 6.8–13.47 g/L, and 5–60 min respectively (Table 1). A total of 20 experiments were carried out based on the experiment design (Table 2). In a typical adsorption experiment, 10 mL aqueous α-toluic acid solution of known concentration was taken in 100 mL Erlenmeyer flask containing a known mass of CaO_2 nanoadsorbent. The flask containing the suspension was kept in a water bath controlled shaker (REMI, RSB-12, India) and shaken at 22 ± 2 °C for a specified time for α-toluic acid adsorption. The suspension was then centrifuged at 3000 rpm for 5 min and the CaO_2 nanoparticles were collected. The supernatant was filtered using 0.45 *μm* filter (Whattman) and the residual CaO_2 nanoparticles were separated. The α-toluic acid concentration in the supernant was determined by NaOH titration using the phenolphthalein indicator [21]. The consistency of the titration was observed within ±2% by repeating the experiments thrice and average values were reported.

The α-toluic acid removal efficiency was calculated as:

$$\%\ \alpha\text{-toluic acid removal} = \frac{(C_0 - C_t)}{C_0} \times 100 \tag{1}$$

where C_0 (g/L) is the initial concentration of α-toluic acid and C_t (g/L) is the α-toluic acid concentration at time *t*, after adsorption.

2.5. Response surface methodology (RSM)

RSM is an effective experimental design technique used to determine the main, quadratic and interactive effects of independent variables on the response [23,24]. It is widely used to improve and optimize the processes. It requires only minimal numbers of experiments to evaluate the interactive effects of multiple variables on the response. The quantitative data obtained from the experiments that were used as input to the RSM to develop a regression model equation were then used to predict the response [25]. In the present work, the central composite design (CCD) of RSM was used to investigate the interactive effects of independent variables on the α-toluic acid removal efficiency (response) using CaO_2 nanoparticle as an adsorbent. The independent variables selected were adsorbent dosage (x_1), initial concentration of α-toluic acid (x_2), and adsorption contact time (x_3). In a 2^3 fractional factorial CCD for three independent variables, the number of experiments (*N*) required to carry out was calculated using the below equation [26]:

$$N = 2^n + 2n + n_c \tag{2}$$

where *n* is the number of independent variables ($n = 3$), n_c is the number of central points ($n_c = 6$). Hence, 20 experiments were performed (see Table 2) to develop a model equation and determine the optimal conditions showing the maximum response. The independent variables were coded with low level as −1 and high level as +1 (Table 1). The axial points kept were (±α, 0, 0), (0, ±α, 0), and (0, 0, ±α), where α is the distance between the axial point and the center point which equals to 1.682 (rotatable).

To predict the response, a quadratic polynomial equation was developed by the RSM involving the interactions of the independent variables:

$$Y = \beta_0 + \sum_{i=1}^{k} \beta_i x_i + \sum_{i=1}^{k} \beta_{ii} x_i^2 + \sum_{i \le i \le j}^{k} \beta_{ij} x_i x_j \tag{3}$$

where *Y* is the predicted response (removal efficiency), β_0 is the model constant, β_i the linear terms, β_{ii} the quadratic terms, β_{ij} the interaction terms, x_i and x_j ($i = 1 \rightarrow 3$: $j = 1 \rightarrow 3$: $i \neq j$) represent the coded form of independent variables.

The relationship below the coded (x_i) and the real values (X_i) is represented as:

$$x_i = \frac{X_i - X_0}{\Delta X} \tag{4}$$

where x_i and x_j are the dimensionless coded values of the independent variables, X_0 is the center point of X_i and ΔX is the step change in X_i. To obtain the quadratic model, each independent variable was varied over levels, i.e., axial points (+ and −) and the center point. Analysis of variance (ANOVA) was performed to evaluate the adequacy of the model, and to determine the coefficients of the individual and the interactive model parameters. Model terms which are of significance were selected based on the *p*-value and *F*-value [27]. The goodness of the quadratic model fit with the experimental α-toluic acid removal efficiency was determined by the correlation coefficient (R^2). Design Expert 7.0.0 was used for the regression analysis, statistical significance of model equations, and optimization of the process variables to achieve the response.

Table 1
Experimental range and the levels of the independent variables.

Independent variables	Range and level	
	Low	High
	−1	+1
CaO_2 adsorbent dosage, g (x_1)	0.008	0.03
Initial α-toluic acid concentration, g/L (x_2)	6.8	13.47
Contact time, min (x_3)	5	60

Table 2
Central composite design of experiments by RSM and α-toluic acid removal efficiency.

Run no.	Experimental design			α-Toluic acid removal (%)	
	Independent variables				
	CaO_2 adsorbent dosage (g) x_1	Initial α-toluic acid concentration (g/L) x_2	Contact time (min) x_3	Experimental	Predicted
1	−1	−1	−1	25.00	29.20
2	+1	−1	−1	93.00	94.54
3	−1	+1	−1	48.99	37.91
4	+1	+1	−1	71.21	65.74
5	−1	−1	+1	45.00	42.07
6	+1	−1	+1	98.00	107.41
7	−1	+1	+1	58.08	50.78
8	+1	+1	+1	81.82	78.61
9	−α	0	0	8.78	19.41
10	+α	0	0	98.65	97.76
11	0	−α	0	89.39	80.32
12	0	+α	0	49.13	63.42
13	0	0	−α	45.27	47.76
14	0	0	+α	70.95	69.41
15	0	0	0	58.78	58.59
16	0	0	0	58.78	58.59
17	0	0	0	58.78	58.59
18	0	0	0	58.78	58.59
19	0	0	0	58.78	58.59
20	0	0	0	58.78	58.59

±α = axial central point = 1.682.

3. Results and discussion

3.1. XRD, TEM and HRTEM analysis of CaO_2 nanoparticles

Fig. 3 shows the XRD of synthesized CaO_2 nanoparticles. The presence of peaks at $2\theta = 30.4^\circ$, 35.9°, 47.7°, 53.5°, and 60.7° implicates the synthesized nanoparticles of CaO_2, as the peak positions are the same as that of standard JCPDS card (No. 03-0865) of CaO_2 [21]. The average particle size (D) of CaO_2 was calculated from the highest intensity peak (002) using the Debye–Scherrer equation [28]:

$$D = K\lambda/(\beta\cos\theta) \tag{5}$$

where K is the Debye–Scherrer constant equal to 0.89, λ is the X-ray wave length equal to 1.5406 Å, β is the full width at half maximum of (002) peak and θ is the Bragg angle (in radians). The calculated average CaO_2 particle size was 16.8 nm.

Fig. 4a shows the size and morphology of CaO_2 nanoparticles examined by TEM. In Fig. 4a the particles are seen spherical, single and isolated which is due to the presence of PEG-200 stabilizers on CaO_2 nanoparticle surface resulting due to steric stabilization in the dispersed form. The observed size range of particles is 5–15 nm, which is in closer agreement with the XRD particle size. Fig. 4b shows the HRTEM image of a single CaO_2 nanoparticle. The presence of multiple planes in a single particle at different orientations suggests that the synthesized CaO_2 nanoparticles are highly polycrystalline in nature.

3.2. Adsorption isotherm

The initial α-toluic acid concentration (C_0) was varied from 6.8 to 13.47 g/L, at a constant contact time of 60 min, with 0.01 g CaO_2 nanoparticles at 25 °C. The equilibrium adsorption capacity of α-toluic acid (q_e) on the CaO_2 nanoadsorbent was calculated as:

$$q_e = \frac{C_0 - C_e}{W} \times V \tag{6}$$

where q_e is the equilibrium capacity of α-toluic acid on the adsorbent (g/g), C_e is the equilibrium concentration of α-toluic acid in solution after adsorption (g/L), V is the volume of solution (L), and W is the mass of CaO_2 nanoparticles in (g). The Freundlich isotherm is applicable to both the monolayer and multilayer adsorption, which assumes that adsorption occurs on heterogeneous surface. The linear form is expressed as [29]:

$$\ln q_e = \ln K_F + \frac{1}{n}\ln C_e \tag{7}$$

where K_F is the Freundlich isotherm constant and n is the Freundlich isotherm exponent. The values of K_F and n were calculated from the intercept and slope of the linear plot of $\ln q_e$ (g/g) versus $\ln C_e$ (g/L) [figure not shown].

The linearized form of Langmuir isotherm model equation is given as below [30]:

$$\frac{C_e}{q_e} = \frac{1}{K_L q_m} + \frac{C_e}{q_m} \tag{8}$$

where q_m is the adsorption capacity of α-toluic acid corresponding to complete monolayer coverage on the CaO_2 surface (g/g) and K_L is the Langmuir adsorption constant (L/g). The q_e values were calculated using Eq. (6). The values of q_m and K_L were determined from the slope and the intercept of the linear plot C_e/q_e versus C_e [figure not shown]. Based on Eq. (8), Langmuir isotherm shows the best fit to the experimental data. Thus, this study confirms that adsorption of α-toluic acid takes place on the CaO_2 nanoparticles, and follows the Langmuir adsorption isotherm model. It assumes

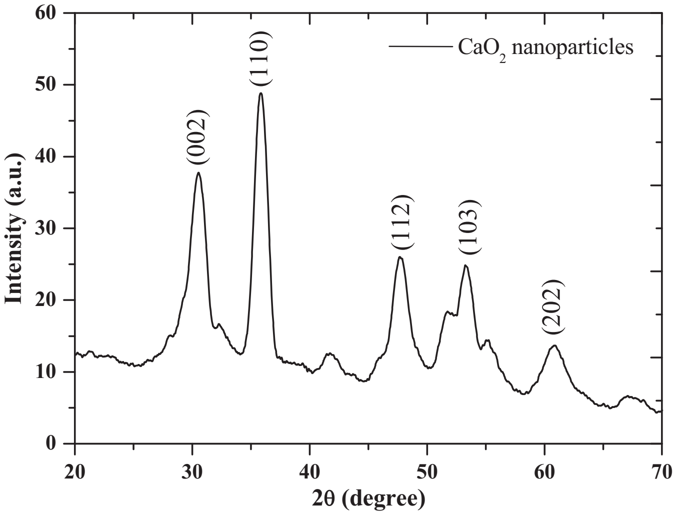

Fig. 3. X-ray diffraction of CaO_2 nanoparticles.

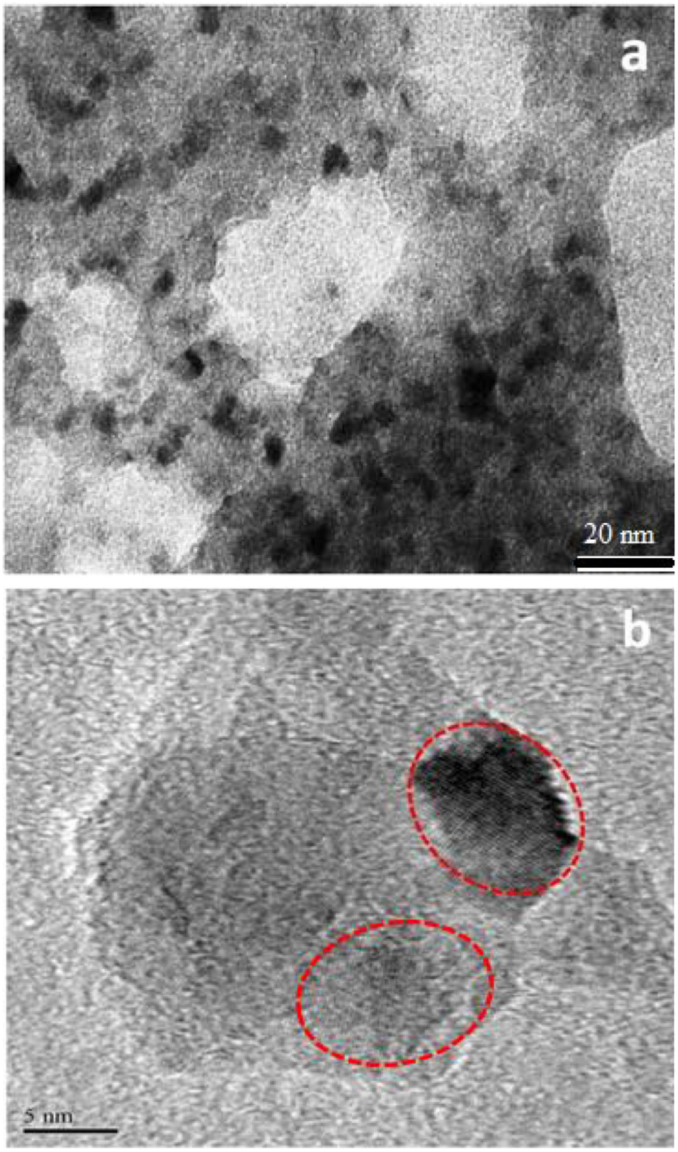

Fig. 4. (a) TEM and (b) HR-TEM images of the PEG-200 coated CaO_2 nanoparticles.

that monolayer adsorption of α-toluic acid takes place over the homogeneous CaO_2 nanoparticle adsorbent surface [31,32].

3.3. Response surface modeling using central composite design

Adsorption experiments were carried out by varying three independent variables' CaO_2 nanoparticle dosage (0.008–0.03 g), initial concentration of α-toluic acid (6.8–13.47 g/L), and contact time (5–60 min) (Table 1). Using CCD, the predicted and the experimental response for varying conditions are shown in Table 2. Based on the sequential model sum of squares, models such as linear, quadratic, cubic models, etc. were listed by the software. Among these, the quadratic model was recommended as it had the highest order polynomial with the additional terms significant, and the model was not aliased.

The quadratic model in terms of coded factors after excluding the insignificant terms is expressed below to predict the response (Y):

$$Y = 20.16 + 4708.92x_1 - 5.21x_2 + 0.23x_3 - 255.69x_1x_2 + 0.42x_2^2 \tag{9}$$

The result of ANOVA test for the model Eq. (9) is summarized in Table 3. A p value less than 0.05 was chosen as the criteria which show the statistical significance of a variable of an effect at 95% confidence level [33]. F value is the ratio of mean square value of each source variable to the residuals [34]. The higher the F value, the greater the significance of the corresponding source variables. Based on F and p values the significant variables x_1, x_2, x_3, x_1x_2, and x_2^2 were selected and the above model Eq. (9) was developed. The correlation between the predicted and the experimental response is shown in Fig. 5. Experimental values are the measured values for a run arranged by the CCD, and the predicted values are from the model Eq. (9). The predicted and the experimental response show a very good agreement with each other, and the coefficient determination (R^2) of 0.92 implicates a good adequacy of the model. Hence, the developed model is capable of relating the response and the significant variables.

The interactive effects of initial concentration of α-toluic acid and CaO_2 adsorbent dosage on the α-toluic acid removal efficiency at a constant contact time of 32.5 min is shown as 3D response surface plot (Fig. 6a). It can be observed that at low adsorbent dosages, the α-toluic acid removal efficiency decreases with increasing the concentration, whereas, at higher adsorbent dosages, the removal efficiency increases with the initial α-toluic acid concentration. The increase in removal efficiency with an increase in adsorbent dosage is attributed to the increase in a number of binding sites of the adsorbent surface. Singh et al. [23] also showed that the Rhodamine B removal efficiency increases with an increase in magnetic nanocomposite (adsorbent) dosage. Similarly, Abdel-Ghani et al. [35] reported that the removal efficiency of lead increases with increasing adsorbents such as rice husk, maize cobs and saw dust. From Fig. 6a, a maximum of 98.65% removal efficiency can be observed at an initial α-toluic acid concentration = 10.135 g/L, and adsorbent dosage = 0.037 at a constant contact time of 32.5 min.

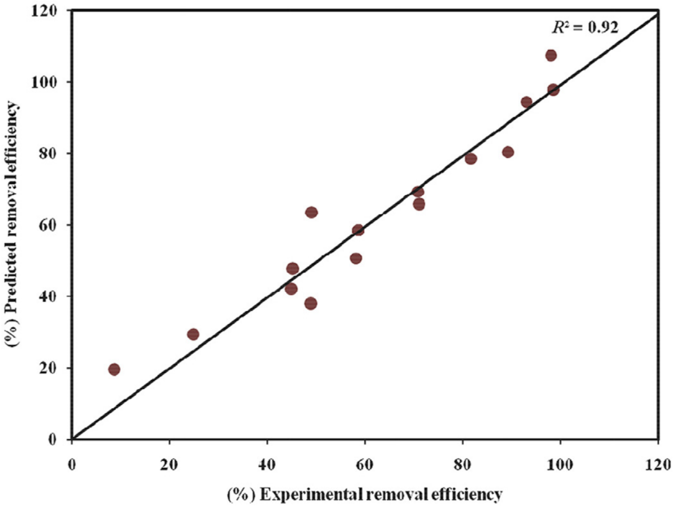

Fig. 5. Correlation of the predicted and the experimental α-toluic acid removal efficiency.

The combined effect of CaO_2 adsorbent dosage and contact time at a constant initial α-toluic acid concentration of 10.135 g/L on the α-toluic acid removal efficiency is shown in Fig. 6b. It could be noted that for both an increase in contact time and the adsorbent dosage the removal efficiency increases. An increase in adsorbent dosage results in more of binding sites available for the α-toluic acid molecules to adsorb, whereas, an increasing contact time provides enough time for the molecules to bind on the adsorbent sites. Similar results were reported by Arulkumar et al. [36] for the Orange G dye removal by adsorption on the activated carbon. Garg et al. [37] showed that the malachite green dye removal efficiency increases with increase in both sawdust and time. From Fig. 6b, a maximum of 98.65% α-toluic acid removal efficiency can be observed at contact time = 32.5 min and adsorbent dosage = 0.037 g for a constant initial α-toluic acid concentration of 10.135 g/L.

Fig. 6c shows the interactive influence of initial α-toluic acid and contact time on the α-toluic acid removal efficiency at a constant CaO_2 adsorbent dosage of 0.019 g. It is evident that at a constant adsorbent dosage, an increase in the initial concentration decreases the removal efficiency. Increasing the contact time did not show any pronounced effect as the rate of adsorption is faster and

Table 3
Analysis of variance (ANOVA) for a response surface quadratic model.

Source	Sum of squares	df	Mean squares	F-value	p-Value	Remark
Model	9347.40	5	1869.48	35.24	<0.0001	Significant
x_1	7409.42	1	7409.42	139.67	<0.0001	Significant
x_2	344.68	1	344.68	6.50	0.0232	Significant
x_3	565.60	1	565.60	10.66	0.0056	Significant
x_1x_2	703.88	1	703.88	13.27	0.0027	Significant
	323.82	1	323.82	6.10	0.0270	Significant
Residual	742.71	14	53.05			
Lack of fit	742.71	9	82.52			
Pure error	0	5	0			
Cor total	10090.11	19				

df = degree of freedom.
$R^2 = 0.92$.

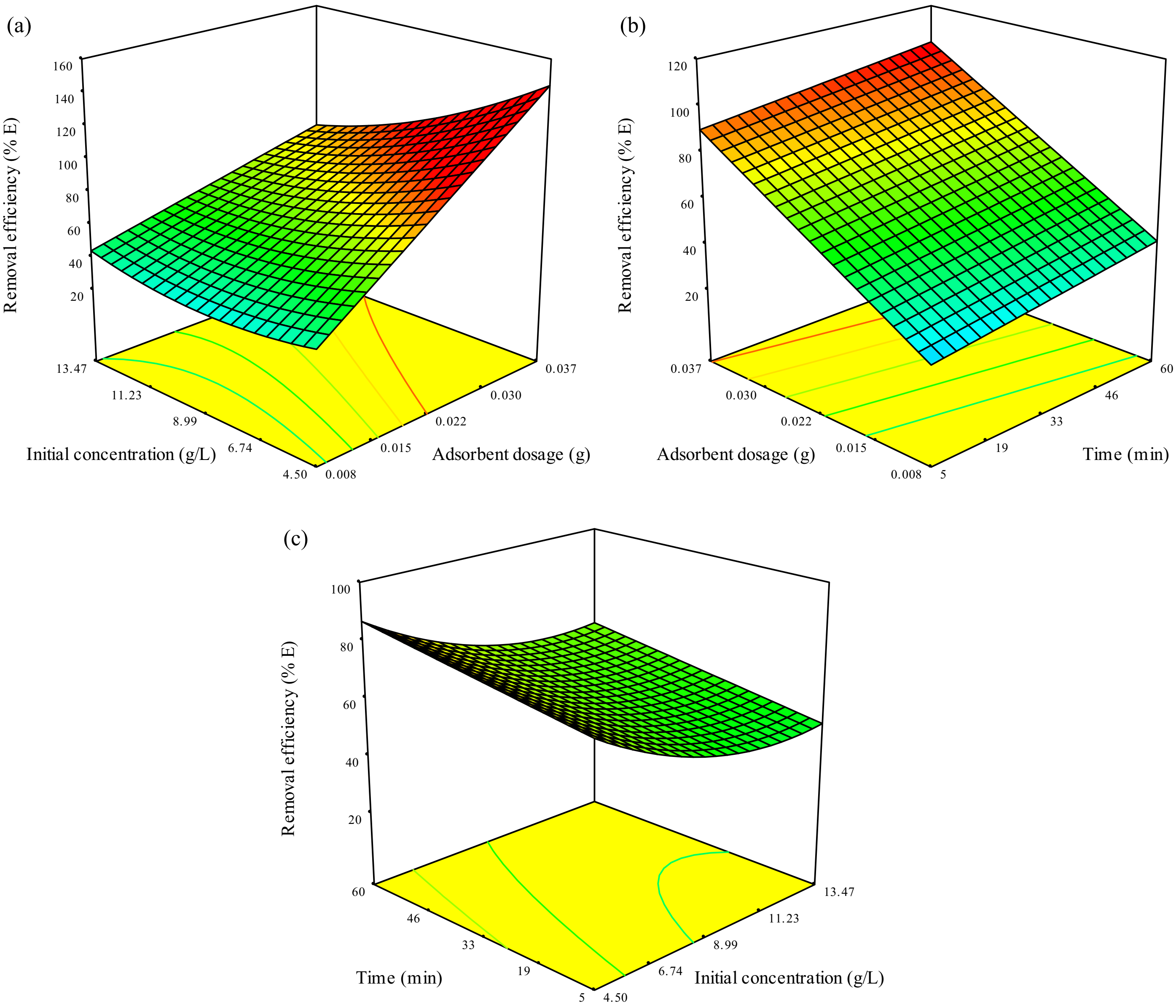

Fig. 6. 3D surface plot showing the effect of (a) CaO_2 adsorbent dosage and the initial α-toluic acid concentration at constant contact time = 32.5 min, (b) contact time and CaO_2 adsorbent dosage at constant initial concentration of α-toluic acid = 10.135 g/L, and (c) initial α-toluic acid concentration and contact time at constant CaO_2 adsorbent dosage = 0.019 g on α-toluic acid removal efficiency (%E).

equilibrium adsorption took place much faster on the limited number of active sites available. Sen [38] also found that the initial concentration of methylene blue dye has more influence on the removal efficiency than the contact time. Similar results were shown by Ansari and Mosayebzad [39] for the removal of methylene blue from aqueous solution using sawdust. From Fig. 6c, a maximum of 89.39% removal efficiency can be observed at an initial α-toluic acid concentration = 10.135 g/L and contact time = 32.5 min for a constant adsorbent dosage of 0.019 g.

From the above, it is to be noted that among the variables' CaO_2 adsorbent dosage, initial concentration of α-toluic acid, and contact time, the interactive effect of adsorbent dosage and initial concentration of α-toluic acid was found to have more influence on the response than the contact time. This implies that the rate of adsorption of α-toluic acid is faster, and the removal efficiency mainly depends on CaO_2 adsorbent dosage and initial concentration of α-toluic acid.

3.4. Optimization of process conditions using desirability function

From Table 2, it can be observed that the response depends on the set of experimental conditions chosen. However, the condition for a specific run is not an optimum order to showing the maximum response. Hence, the optimization of process has to be carried out to determine the optimal conditions showing maximum response. To achieve this, numerical optimization using Design Expert 7.0.0 was performed. Desirability function ranging from 0.0 to 1.0 was set as the criteria for determining the optimum conditions showing the maximum response. A desirability function value closer to 1 gives the optimized conditions with a maximum response [40]. The overall desirability function depends on the goal set. The goals are "maximize, minimize, target, is in range, and none." In our case, the goal "is in range" was set for each independent variable with a lower limit and a higher limit. The goal "maximize" was set for the response. The lower limit for the CaO_2

Table 4
Conditions set to determine the overall desirability functions for optimization of α-toluic acid removal via adsorption using CaO_2 nanoparticles.

Name	Goal	Lower limit	Upper limit	Lower weight	Upper weight	Importance
CaO_2 adsorbent dosage (g)	Is in range	0.008	0.03	1	1	3
Initial α-toluic acid concentration (g/L)	Is in range	6.8	13.47	1	1	3
Contact time (min)	Is in range	5	60	1	1	3
Response (α-toluic acid removal efficiency, %)	Maximize	8.78	98.65	1	1	3

Table 5
Comparison of RSM predicted and the experimental α-toluic acid removal efficiency (in %) at the optimal conditions.

CaO_2 adsorbent dosage (g)	Initial α-toluic acid concentration (g/L)	Contact time (min)	Predicted removal efficiency (%)	Experimental removal efficiency (%)
0.03	7.06	34	99.50	98.05

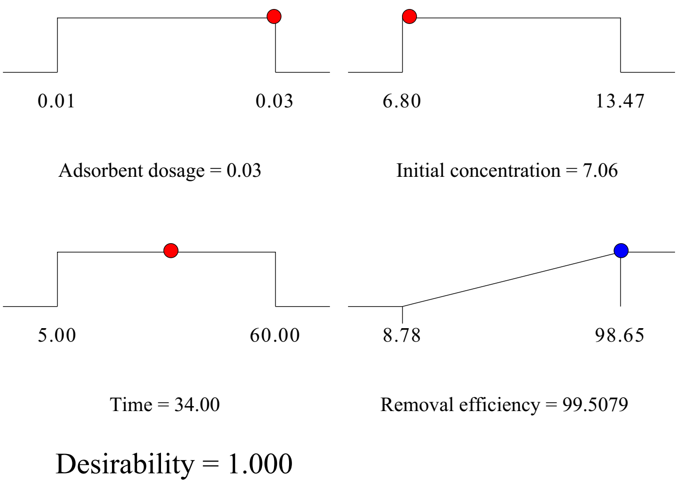

Fig. 7. Desirability ramp obtained from the numerical optimization.

adsorbent dosage, initial concentration of α-toluic acid, and contact time kept were 0.008 g, 6.8 g/L, and 5 min respectively. The higher limit for the CaO_2 adsorbent dosage, initial concentration of α-toluic acid, and contact time kept were 0.03 g, 13.47 g/L, and 60 min respectively. The upper and the lower weights (used to adjust the shape of desirable function) for each goal was set as 1. Table 4 shows all the conditions set to determine the overall desirability function. To achieve the goals, the programs begin at a random starting point and proceed up the steepest slope to a maximum. The numerical optimization gave a point where the desirability function was 1. At this point, the best local maximum from the ramp desirability function for each independent variable was found (Fig. 7). From this study, the desired optimal conditions for the CaO_2 adsorbent dosage, initial concentration of α-toluic acid, contact time and the target response were found to be 0.03 g, 7.06 g/L, 34 min and 99.50% respectively.

In order to validate the predicted optimal conditions, experiments were carried out under these conditions and 98.05% α-toluic acid removal efficiency was achieved. Table 5 shows the comparison of predicted and the experimental response at the optimal conditions. A good agreement between the predicted and the experimental response confirms the adequacy of the model.

4. Conclusion

CaO_2 nanoparticles were prepared by chemical precipitation method and characterized using different techniques XRD, TEM, and HR-TEM. CCD proved to be very effective in predicting the α-toluic acid removal efficiency. The model showed that the initial concentration of α-toluic acid and CaO_2 adsorbent dosage has more influence on α-toluic acid removal efficiency than the contact time. ANOVA test showed the significance of the developed RSM model. The predicted optimal conditions for CaO_2 adsorbent dosage, initial concentration of α-toluic acid, and contact time were found to be 0.03 g, 7.06 g/L, and 34 min respectively, which showed experimental removal efficiency up to 98.05%. Comparison of the model predicted and experimental response gave R^2 of 0.92, proving the model as efficient in determining the α-toluic acid removal efficiency using CaO_2 nanoparticles as an adsorbent. CaO_2 nanoparticles were used as adsorbent for effective removal α-toluic acid from its aqueous solution.

Acknowledgement

We thank Ministry of Human Resource Development, Government of India, for the financial support. We gratefully thank SAIF IIT Bombay for carrying out the TEM facility and SAIF NEHU Shillong for providing the HRTEM facility. We also thank Metallurgical & Materials Engineering Department, VNIT for providing the XRD facility.

References

[1] R. Adams, A.F. Thal, Phenylacetic acid, Org. Synth 2 (1922) 436.
[2] W. Wenner, Org. Synth 32 (1952) 760.
[3] K. Ramchandran, S.A. Krishnamurthy, S.H. Subbaraman, J. Chem. Technol. Biotechnol 66 (1996) 243–250.
[4] R. Shrivastava, H. Purohit, P.S. Phale, Metabolism and preferential utilization of phenylacetic acid and 4-hydroxyphenylacetic acid in pseudomonas putida CSV86, J. Bioremed. Biodegrad 2 (2011) 120.
[5] J. Gunjan, D. Awadh, Synthesis and biological evaluation of some phenyl acetic acid hydrazone derivatives, Int. Res. J. Pharm 2 (2011) 110–112.
[6] S.H. Kim, J.L. Yang, Y.S. Song, Physiological functions of chungkuk-jang, Food Nutr. Res 4 (1999) 40–46.
[7] H.K. Yong, H.S. Choi, S.H. Hur, J.H. Hong, Antimicrobial activities of viscous substances from chungkukjang fermented with different bacillus ssp, J. Food Hyg. Saf 16 (2001) 288–293.
[8] K.L. Wasewar, D.Z. Shende, Extraction of caproic acid using tri-n-butyl phosphate in benzene and toluene at 301, J. Chem. Eng. Data 55 (2010) 4121–4125.
[9] H. Uslu, I. Inci, S.S. Bayazi, Adsorption equilibrium data for acetic acid and glycolic acid onto amberlite IRA-67, J. Chem. Eng. Data 55 (2010) 1295–1299.
[10] S.D. Mamadou, N. Savage, Nanoparticles and water quality, J. Nano. Res 7 (2005) 325–330.
[11] X.L. Zhao, Y.L. Shi, Y.Q. Cai, S.F. Mou, Cetyltrimethylammonium bromide-coated magnetic nanoparticles for the pre-concentration of phenolic compounds from environmental water samples, Environ. Sci. Technol 142 (2008) 1201–1206.
[12] H.M. Kalavathy, I. Regupathi, M.G. Pillai, L.R. Miranda, Modelling, analysis and optimization of adsorption parameters for H_3PO_4 activated rubber wood sawdust using response surface methodology (RSM), Colloids Surf. B Biointerfaces 70 (1) (2009) 35–45.
[13] E. Olyaie, H. Banejad, A. Afkhami, A. Rahmani, J. Khodaveisi, Development of a cost-effective technique to remove the arsenic contamination from aqueous solutions by calcium peroxide nanoparticles, Sep. Purif. Technol 95 (2012) 10–15.
[14] Y. Qian, X. Zhou, Y. Zhang, W. Zhang, J. Chen, Performance and properties of nanoscale calcium peroxide for toluene removal, Chemosphere 91 (2013) 717–723.
[15] B. Karn, T. Kuiken, M. Otto, Nanotechnology and in situ remediation: a review of the benefits and potential risks, Environ. Health Perspect 117 (2009) 1813–1831.

[16] U.K. Garg, M.P. Kaur, V.K. Garg, D. Sud, Removal of Nickel (II) from aqueous solution by adsorption on agricultural waste biomass using a response surface methodological approach, Bioresour. Technol 99 (2008) 325.

[17] M. Sarkar, P. Majumdar, Application of response surface methodology for optimization of heavy metal biosorption using surfactant modified chitosan bead, Chem. Eng. J. 175 (2011) 376–387.

[18] M.Z. Alam, S.A. Muyibi, J. Toramae, Statistical optimization of adsorption processes for removal of 2,4-dichlorophenol by activated carbon derived from oil palm empty fruit bunches, J. Environ. Sci 19 (2007) 674–677.

[19] G. Annadurai, R.S. Juang, D.J. Lee, Factorial design analysis of adsorption of activated carbon on activated carbon incorporated with calcium alginate, Adv. Inorg. Environ. Res 6 (2002) 191–198.

[20] N. Aslan, Application of response surface methodology and central composite rotatable design for modeling and optimization of a multi-gravity separator for chromite concentration, Powder Technol 185 (2008) 80–86.

[21] S.S. Madan, A.W. Upwanshi, K.L. Wasewar, Adsorption of α-toluic acid by calcium peroxide nanoparticles, Des. Water Treat 57 (2016) 16507–16513.

[22] J. Khodaveisi, H. Banejad, A. Afkhami, E. Olyaie, S. Lashgari, R. Dashti, Synthesis of calcium peroxide nanoparticles as an innovative reagent for in situ chemical oxidation, J. Hazard. Mater 192 (2011) 1437–1440.

[23] K.P. Singh, S. Gupta, A.K. Singh, S. Sinha, Experimental design and response surface modeling for optimization of rhodamine B removal from water by magnetic nanocomposite, Chem. Eng. J. 165 (2010) 151–160.

[24] K. Karthikeyan, K. Nanthakumar, K. Shanthi, P. Lakshmanaperumalsamy, Response surface methodology for optimization of culture conditions for dye decolorization by a fungus, Aspergillus niger HM11 isolated from dye affected soil, Iran. J. Microbiol 2 (2010) 213–222.

[25] E. Rodríguez-Carmona, A. Manresa, J. Bastida, Application of experimental design and canonical analysis of response surfaces to the optimization of poly (3-hydroxyalkanoates) production by Pseudomonas aeruginosa 42A2, Chem. Biochem. Eng. Q. 27 (2013) 457–465.

[26] I.A.W. Tan, A.L. Ahmad, B.H. Hameed, Preparation of activated carbon from coconut husk: optimization study on removal of 2,4,6-trichlorophenol using response surface methodology, J. Hazard. Mater 153 (2008) 709–717.

[27] K. Ravikumar, K. Pakshirajan, T. Swaminathan, K. Balu, Optimization of batch process parameters using response surface methodology for dye removal by a novel adsorbent, Chem. Eng. J. 105 (2005) 131–138.

[28] V.K. Gupta, A. Nayak, Cadmium removal and recovery from aqueous solutions by novel adsorbents prepared from orange peel and Fe_2O_3 nanoparticles, Chem. Eng. J. 180 (2012) 81–90.

[29] H.M.F. Freundlich, Over the adsorption in solution, J. Phys. Chem 57 (1906) 385–470.

[30] I. Langmuir, The adsorption of gases on plane surfaces of glass, mica and platinum, J. Am. Chem. Soc 40 (1918) 1361–1403.

[31] S.S. Madan, K.L. Wasewar, C.R. Kumar, Adsorption kinetics, thermodynamics, and equilibrium of a-toluic acid onto calcium peroxide nanoparticles, Adv. Powder Technol (2016). http://dx.doi.org/10.1016/j.apt.2016.07.024.

[32] S.S. Madan, K.L. Wasewar, S.L. Pandharipande, Modeling the adsorption of benzeneacetic acid on CaO_2 nanoparticles using artificial neural network, Res. Effi. Technol (2016). http://dx.doi.org/10.1016/j.reffit.2016.10.004.

[33] M. Jain, V.K. Garg, K. Kadirvelu, Investigation of Cr (VI) adsorption onto chemically treated Helianthus annuus: optimization using response surface methodology, Bioresour. Technol 102 (2011) 600–605.

[34] K.M. Desai, S.A. Survase, P.S. Saudagar, S.S. Lele, R.S. Singhal, Comparison of artificial neural network (ANN) and response surface methodology (RSM) in fermentation media optimization: case study of fermentative production of scleroglucan, Biochem. Eng. J. 41 (2008) 266–273.

[35] N.T. Abdel-Ghani, M. Hefny, G.A.F. El-Chaghaby, Removal of lead from aqueous solution using low cost abundantly available adsorbents, Int. J. Environ. Sci. Technol 4 (2007) 67–73.

[36] M. Arulkumar, P. Sathishkumar, T. Palvannan, Optimization of orange G dye adsorption by activated carbon of Thespesia populnea pods using response surface methodology, J. Hazard. Mater 186 (2011) 827–834.

[37] V.K. Garg, R. Gupta, A.B. Yadav, R. Kumar, Dye removal from aqueous solution by adsorption on treated sawdust, Bioresour. Technol 89 (2003) 121–124.

[38] T.K. Sen, Removal of cationic dye methylene blue (MB) from aqueous solution by adsorption on biosolid adsorbent, Int. J. Environ. Pollut. Control Manage 3 (1) (2011) 1–10.

[39] R. Ansari, Z. Mosayebzad, Removal of basic dye methylene blue from aqueous solutions using sawdust and sawdust coated with polypyrrole, J. Iran. Chem. Soc 7 (2) (2010) 339–350.

[40] M. Vaez, A.Z. Moghaddam, S. Alijani, Optimization and modeling of photocatalytic degradation of azo dye using a response surface methodology (RSM) based on the central composite design with immobilized titania nanoparticles, Ind. Eng. Chem. Res 51 (2012) 4199–4207.